NASA TECHNICAL MEMORANDUM

NASA TM 73717

NASA TM 73717

THREE-DIMENSIONAL ELASTIC STRESS AND DISPLACEMENT ANALYSIS OF FINITE GEOMETRY SOLIDS CONTAINING CRACKS

by Jonathan Kring, John Gyekenyesi,
and Alexander Mendelson
Lewis Research Center and
U.S. Army Air Mobility R&D Laboratory
Cleveland, Ohio 44135

TECHNICAL PAPER presented at the
Twenty-third Conference of Army Mathematicians
sponsored by the Department of the Army
Hampton, Virginia, May 11-13, 1977

THREE-DIMENSIONAL ELASTIC STRESS AND DISPLACEMENT ANALYSIS OF FINITE GEOMETRY SOLIDS CONTAINING CRACKS

Jonathan Kring, John Gyekenyesi, and Alexander Mendelson
Lewis Research Center and
U.S. Army Air Mobility R&D Laboratory
Cleveland, Ohio 44135

ABSTRACT. The line method of analysis is applied to the Navier-Cauchy equations of elastic equilibrium to calculate the displacement fields in finite geometry bars containing central, surface, and double-edge cracks under extensionally applied uniform loading. The application of this method to these equations leads to coupled sets of simultaneous ordinary differential equations whose solutions are obtained along sets of lines in a discretized region. Normal stresses and the stress intensity factor variation along the crack periphery are calculated using the obtained displacement field. The reported results demonstrate the usefulness of this method in calculating stress intensity factors for commonly encountered crack geometries in finite solids.

INTRODUCTION. The main goal of fracture mechanics is the prediction of the load at which a structure weakened by a crack will fail. Knowledge of the stress and displacement distributions near the crack tip is of fundamental importance in evaluating this load at failure. During the early development of crack mechanics most of the effort was focused on through-thickness cracks which could be characterized as two-dimensional. However, part-through cracks are the most common type of crack defect found in actual service conditions (ref. 1).

E-9263

Because of the geometric singularity associated with any crack type problem, only limited analytical work has been done in the past on these problems. Early theoretical solutions for three-dimensional flaw configurations usually involved the discussion of cracks in infinite or semi-infinite solids (refs. 2 to 8). For this reason, results for finite geometry stress intensity factors are usually given in terms of magnification factors applied to some convenient reference solution. In addition, considerable scatter exists in the reported results as obtained by different investigators (ref. 9). In our work these difficulties are avoided by solving the finite dimensional problems directly.

Recently, approximate solutions of the finite geometry surface crack problem were obtained by the boundary integral equation method (ref. 10) and the finite element method (ref. 11). An alternate semi-analytical method suitable for the elastic solution of crack problems is the line method of analysis. Successful application of this method to finite geometry solids containing cracks has been demonstrated by Gyekenyesi and Mendelson (ref. 12). Although the concept of the line method for solving partial differential equations is not new (ref. 13), its application in the past has been limited to simple examples. The basis of this technique is the substitution of finite differences for the derivatives with respect to all the independent variables except one for which

the derivatives are retained. This approach replaces a given partial differential equation with a system of simultaneous ordinary differential equations whose solutions can then be obtained in closed form. These equations describe the dependent variable along lines which are parallel to the coordinate in whose direction the derivatives were retained. Application of the line method is most useful when the resulting ordinary differential equations are linear and have constant coefficients.

An inherent advantage of the line method over other numerical methods is that good results are obtained from the use of relatively coarse grids. This use of a coarse grid is permissible because parts of the solutions are obtained in terms of continuous functions. Additional accuracy in normal stress distributions is derived from the fact that they are expressed as first-order derivatives of the displacements and these derivatives can be analytically evaluated. Inherently inaccurate numerical differentiation is required only for evaluating the shear stresses, but this presents no important loss of accuracy since they are an order of magnitude smaller than the normal stresses. For problems with geometric singularities, additional accuracy is derived from using a displacement formulation since the resulting deformations are not singular.

It is the purpose of this report to present a simple and systematic approach to the elastic analysis of three-dimensional, finite geometry solids containing traction-free cracks. The need for these specific solutions has existed for a number of years in fracture toughness testing.

REDUCTION OF THE NAVIER-CAUCHY EQUATIONS TO SYSTEMS OR ORDINARY DIFFERENTIAL EQUATIONS. Within the framework of linearized elasticity theory, the equations of elastic equilibrium in terms of displacements are

$$(\lambda + G)\frac{\partial e}{\partial x} + G\nabla^2 u = 0 \tag{1}$$

$$(\lambda + G)\frac{\partial e}{\partial y} + G\nabla^2 v = 0 \tag{2}$$

$$(\lambda + G)\frac{\partial e}{\partial z} + G\nabla^2 w = 0 \tag{3}$$

where the body forces are assumed to be zero and the dilatation is

$$e = \frac{\partial u}{\partial x} + \frac{\partial v}{\partial y} + \frac{\partial w}{\partial z} \tag{4}$$

For a finite geometry solid with rectangular boundaries, we construct three sets of parallel lines (fig. 1(a)). Each set of lines is parallel to one of the coordinate axes and thus perpendicular to the corresponding coordinate plane. An approximate solution of equation (1) can be obtained by developing solutions of ordinary differential equations along the x-directional lines. As seen in the figure, ther are a total of $\iota = NY \times NZ$ such lines where NY is the number of lines along the y-direction and NZ is the number of lines along the z-direction in a given plane, respectively. We define the displacements along these lines as $u_1, u_2, \ldots, u_\iota$. The derivatives of the y-directional displacements on these lines with respect to y are defined as $v'|_1, v'|_2, \ldots, v'|_\iota$, and the derivatives of the z-directional displacements with respect to z are defined as $w'|_1, w'|_2, \ldots, w'|_\iota$. These displacements and derivatives can then be regarded as functions of x only since they are variables on x-directional lines. When these definitions are used, the ordinary differential equation along a generic line ij (a double subscript is used here for simplicity of writing) in figure 1(b) may be written as

$$\frac{d^2u_{ij}}{dx^2} + \frac{(1-2\nu)}{2(1-\nu)}\left[-\left(\frac{2}{h_y^2}+\frac{2}{h_z^2}\right) + \frac{1}{h_y^2}(u_{i+1,j}+u_{i-1,j}) + \frac{1}{h_z^2}(u_{i,j+1}+u_{i,j-1})\right] + \frac{f_{ij}(x)}{2(1-\nu)} = 0 \qquad (5)$$

where

$$f_{ij}(x) = \left.\frac{dv'}{dx}\right|_{ij} + \left.\frac{dw'}{dx}\right|_{ij} \qquad (6)$$

and

$$v' = \frac{dv}{dy}, \quad w' = \frac{dw}{dz}$$

Similar differential equations are obtained along the other x-directional lines. Since each equation has the terms of the displacements on the surrounding lines, these equations constitute a system of ordinary differential equations for the displacements $u_1, u_2, \ldots, u_\iota$.

The set of ι second order differential equations represented by (5) can be reduced to a set of 2ι first order differential equations by treating the derivatives of the u's as an additional set of ι unknowns, i.e., defining

$$u_{i+1} = \frac{du_1}{dx}, \quad u_{i+2} = \frac{du_2}{dx}, \text{ etc.} \tag{7}$$

The resulting $2i$ equations can now be written as a single first order matrix differential equation

$$\frac{du}{dx} = A_1 U + R(x) \tag{8}$$

where U and R are column matrices of $2i$ elements each and A_1 is a $2i \times 2i$ matrix of the constant coefficients appearing in equations (5) and (7).

In a similar manner, to solve equations (2) and (3), ordinary differential equations are constructed along the y- and z-directional lines respectively. These equations are also expressed in an analogous form to equations (8); they are

$$\frac{dV}{dy} = A_2 V + S(y) \tag{9}$$

$$\frac{dw}{dz} = A_3 W + T(z) \tag{10}$$

Equations (8) to (10) are linear first-order ordinary matrix differential equations. They are, however, not independent, but are coupled through the vectors, R, S and T whose components are given by equations similar to (6). The elements of the coefficient matrices A_1, A_2, and A_3 are all constants, being functions of the mesh spacing and Poisson's ratio only.

Noting that a second-order differential equation can satisfy only a total of two boundary conditions and since three-dimensional elasticity problems have three boundary conditions at every point of the bounding surface, some of the boundary data must be incorporated into the surface line differential equations. Hence, conditions of normal stress and displacement are enforced through the constants of the homogeneous solutions while shear stress boundary data must be incorporated into the differential equations of the surface lines. The application of the specified shear conditions permits the use of central difference approximations when surface line differential equations are constructed. The details of constructing these equations are found in reference 14.

SOLUTION OF THE SYSTEMS OF ORDINARY DIFFERENTIAL EQUATIONS. The systems of ordinary differential equations (8) to (10) can be solved by any of a number of standard techniques. The method used herein was basically the matrizant or Peano-Baker method of integration (ref. 15). For equation (8) the solution can be written as

$$U(x) = e^{A_1 x} U(0) + e^{A_1 x} \int_0^x e^{-A_1 \eta} R(\eta)\, d\eta \qquad (11)$$

with similar solutions for equations (9) and (10). U(0) is the initial value vector, determined from the boundary conditions. The conversion of given boundary data into required initial values is discussed in more detail in reference 14.

The matrizant $e^{A_1 x}$ is generally evaluated by its matrix series. For larger values of x, when convergence becomes slow, additive formulas may be used. In addition, similarity transformations can be used to diagonalize the matrix A_1. These various techniques for improving the accuracy are discussed in detail in reference 14.

Since equations (8) to (10) and their boundary conditions are highly coupled, it is generally impossible to directly evaluate their solutions. Thus, a successive approximation procedure must be employed where assumed values must be used initially for the required unknowns. The cyclic resubstitution of the obtained solutions into the coupling vectors and the boundary conditions will usually converge to the correct solution, depending mainly on the accuracy to which the required matrizant can be evaluated.

Once the successive approximation procedure has converged and the displacement field in the body has been calculated, the normal stress distributions can be obtained directly by using the stress-displacement equations. The shear stresses, however, can be evaluated only through finite difference approximations for the required displacement gradients.

STRESS INTENSITY FACTOR. The stress intensity factor K_I was at first obtained from the calculated stresses and displacements by extending the usual definition

$$K_I = \lim_{R \to 0} \sigma_y (2\pi R)^n \qquad (12)$$

to discrete data, where R is measured from and is normal to the crack front and n is the singularity. It was found, however, that due to the coarseness of the grid used, the usual plotting and extrapolating techniques gave results that were erratic and of questionable accuracy. This was compounded by the fact that the precise crack tip location is not really known except that it is approximately midway between two lines, one of which has zero displacement specified in the crack plane and one of which has zero stress specified. It was found, however, that by using two terms in the stress and displacement series expansions around the crack tip, good results could be obtained even with the coarse grid used. Furthermore, this also permitted us to determine the actual crack tip location from the computed results. The method utilized is as follows. We take

$$v\Big|_{y=0} = \alpha K_I \left[\sqrt{\frac{R + r}{2\pi}} + \frac{L_I}{K_I} \sqrt{(R + r)^3} \right] \tag{13}$$

$$\sigma_y\Big|_{y=0} = K_I \left[\frac{1}{\sqrt{2\pi(R - r)}} + \frac{L_I}{K_I} \sqrt{R - r} \right] \tag{14}$$

where α is a function of Poisson's ratio, n was assumed to be -1/2 and r is the crack edge position correction measured from the originally assumed midpoint position. Using displacement data from three adjacent nodes to the crack edge in equation (13), values of αK_I, L_I/K_I, and r are calculated for each value of z, with R also measured from the half-way point between nodes specifying boundary stresses and displacements, respectively. Substituting values of L_I/K_I and r into equation (14), we can calculate K_I as a function of the corrected crack edge distance, $\rho = R - r$. A plot of ln K_I versus $\sqrt{\rho}$ as $\sqrt{\rho} \to 0$ can then be used to obtain K_I. In a similar manner, α can now be calculated from equation (13), where the corrected crack edge distance with the displacement data is $\rho = R + r$.

APPLICATION TO TENSILE FRACTURE SPECIMENS CONTAINING CRACKS. A great amount of experimental work has been done in fracture mechanics (ref. 16) through the use of crack-notched specimens. In the past, many different types of specimens have been used to determine a material's fracture toughness. The most common early specimens employed in these tests were the center-cracked and double-edge-notched bar specimens. Figures 2(a) and 3(a) show the finite rectangular bars with through-thickness, traction-free central and double-edge cracks, respectively. Because of the symmetric geometry and loading, only one-eighth of each bar has to be discretized as shown in figures 2(b) and 3(b).

NUMERICAL RESULTS. - Center-Cracked Tensile Fracture Specimen. The solution of this problem was obtained by using two different sets of lines along the coordinate axes so that the convergence of the finite difference approximations could be checked. In a given direction, uniform line spacing was used in all computations with no other restriction being placed on the selection of the grid size. The crack edge location with respect to the imposed grid was initially assumed to be halfway between nodes specifying normal stress and displacement boundary conditions, respectively. Subsequently, using the obtained near crack tip stresses and displacements, a more accurate crack edge location was established for calculating the stress intensity factor. This approach was considered acceptable since the results from the two sets of lines at corresponding points did not change, although the crack edge to node distance was considerably decreased for the finer mesh. The successive approximation procedure required for decoupling the three sets of ordinary differential equations was terminated when the difference between successively calculated nondimensionalized displacements, which are of the order of unity, at every point was less than a present value (10^{-6}). As expected, the convergence rate of this

successive approximation procedure was greatly dependent on the initial guess for the required unknowns in the coupling vectors and boundary conditions. For maximum computer efficiency, displacement data obtained from the use of coarse grids was interpolated to obtain improved starting values for the computations involving the final spacing of lines. The required initial quantities for the preliminary coarse grid calcualtions were taken to be zero in our work. All calculations were performed on a UNIVAC 1100/40 computer, using double precision arithmetic.

For the selected geometry, the crack opening displacements and normal stresses from our analysis and those from Raju's finite element method (ref. 17) are compared in Table I. Although in our solution of the gross displacement and stress fields, the minimum corrected crack edge distance is $\rho = 0.042c$, crack opening displacements and stresses can be calculated from equations (13) and (14) at any value of ρ for which these equations are assumed to be accurate ($\rho = 0.40c$ or less in this problem). As seen from Table I, there is good agreement in most displacements, with the normal stress at the surface showing the greatest difference.

The dimensionless crack opening displacement is shown in figure 4. Agreement with the finite element results is seen to be very good. It is noteworthy that the results correspond to elliptical crack profiles in all cases.

An indication of the accuracy of our technique for computing the stress intensity factor is seen in figure 5. This figure shows the stress intensity factor variation across the bar thickness. The results obtained in reference 17 using a finite elements method for a geometry almost identical to one of the geometries in this paper is also shown. It is seen that very good agreement is obtained between two completely different methods. In addition, Isida's plane solution (ref. 18), corrected for finite width and length, is also shown in this figure for comparison. Note that these results indicate a small increas in K_I at the surface with increasing bar thickness. Interestingly, for bars with $t > 3c$, K_I increases gradually with z, reaching a maximum near $z = 0.85t$, and then decreases rapidly to its surface value.

Surface Crack Tensile Fracture Specimen. Figure 6 shows a finite geometry bar containing a traction free rectangular surface crack. Because of the symmetric geometry and loading, only one-fourth of the bar has to be discretized as shown in figure 6(b).

Selected results of the dimensionless surface crack opening displacements are shown in figure 7. Note that the crack opening increases rapidly with crack depth for $0.21 \leq a/t \leq 0.87$, slightly exceeding even the surface crack displacement of a through-thickness crack at $a/t = 0.87$. The plane strain solution for a finite width center cracked bar is also shown in figure 7 for reference. Final displacement values in this report were obtained from a set of 100, 140, and 140 x-, y-, and z-directional differential equations, respectively. A typical computer run for this system of equations takes approximately 30 to 40 minutes of CPU time and 720 K bytes of storage.

In order to show the singularity of the stresses, the y-directional normal stress in the crack plane is plotted in figure 8 for $a/t = 0.536$. The results clearly indicate the singular nature of σ_y along the crack periphery.

Double Edge Crack Tensile Fracture Specimen. Our last example is the finite bar with double edge cracks. The crack opening displacements for this problem are presented in figure 9. The stress intensity factor variation as a function of bar thickness is shown in figure 10. In both, results from the finite element method are shown for comparison. Agreement is again excellent.

CONCLUSIONS. The line method of analysis presented affords a practical way for analysis of three-dimensional crack problems, at least for bodies with reasonably regular boundaries. Because parts of the solution are obtained as continuous functions along the lines chosen, relatively good accuracy can be obtained with coarse grids. Results of the analysis include the displacements and normal stresses at every node inside the body from which the stress intensity factor variations were easily calculated. In addition it should be noted that the common semi-elliptical surface crack problem could also be analyzed by merely changing the boundary conditions at certain nodes in the crack plane. Introduction of plasticity into the analysis could also be accomplished by changing the coupling terms in equations (8) to (10). Since these have to be determined by an interative process in any case, it would seem possible to solve the elastoplastic problem by a simple extension of the present method. Whether this approach is practical requires further investigation.

REFERENCES

1. Srawley, John E.; and Esgar, Jack B.: Investigation of Hydrotest Failure of Thiokol Chemical Corporation 260-Inch-Diameter SL-1 Motor Case. NASA TM X-1194, 1966.

2. Irwin, G. R.: Crack-Extension-Force for a Part-Through Crack in a Plate. J. Appl. Mech. vol. 29, no. 4, Dec. 1962, pp. 651-654.

3. Smith, Fred. W.: Stresses Near a Semi-Circular Edge Crack. Ph.D. Thesis, Univ. Washington, 1966.

4. Smith, F. W.; and Alavi, M. J.: Stress Intensity Factors for a Part-Circular Surface Flaw. Proceedings of the First International Pressure Vessel Conference, Holland, 1969.

5. Thresher, R. W.; and Smith, F. W.: Stress-Intensity Factors for a Surface Crack in a Finite Solid. J. Appl. Mech., vol. 39, no. 1, Mar. 1972, pp. 195-200.

6. Shah, R. C.; and Kobayashi, A. S.: Stress Intensity Factor for an Elliptical Crack Under Arbitrary Normal Loading. J. Eng. Fract. Mech., vol. 3, July 1971, pp. 71-96.

7. Shah, R. C.; and Kobayashi, A. S.: On the Surface Flaw Problem. The Surface Crack: Physical Problem and Computational Solutions. Am. Soc. Mech. Eng., 1972, pp. 79-124.

8. Hartranft, R. J.; and Sih, G. C.: Alternating Method Applied to Edge and Surface Crack Problems. Methods of Analysis and Solutions of Crack Problems: Recent Developments in Fracture Mechanics; Theory and Methods of Solving Crack Problems. Leiden, Noordhoff International Publ., 1973, pp. 179-238.

9. Keays, R. H.: A Review of Stress Intensity Factors for Surface and Internal Cracks. ARL/SM-Rept-343, Aeronautical Res. Labs., 1973.

10. Cruse, T. A.: Numerical Evaluation of Elastic Stress Intensity Factors by the Boundary-Integral Equation Method. The Surface Crack: Physical Problems and Computational Solutions. Am. Soc. Mech. Eng., 1972, pp. 153-170.

11. Marcal, P. V.: Three-Dimensional Finite Element Analysis for Fracture Mechanics. The Surface Crack: Physical Problems and Computational Solutions. Am. Soc. Mech. Eng., 1972, pp. 187-202.

12. Gyekenyesi, J. P.; and Mendelson, A.: Three-Dimensional Elastic Stress and Displacement Analysis of Finite Geometry Solids Containing Cracks. Int. J. Fract., vol. II, no. 3, June 1975, pp. 409-429.

13. Jones, D. J.; South, J. C.; and Klunker, E. B.: On the Numerical Solution of Elliptic Partial Differential Equations by the Method of Lines. J. Comput. Phys., vol. 9, 1972, pp. 496-527.

14. Gyekenyesi, J. P.: Solution of Some Mixed Boundary Value Problems of Three-Dimensional Elasticity by the Method of Lines. Ph.D. Thesis, Michigan State Univ., 1972.

15. Frazer, R. A.; Duncan, W. J.; and Collar, A. R.: Elementary Matrices and Some Applications to Dynamic and Differential Equations. Cambridge Univ. Press, 1938.

16. Sih, G. C.: Handbook of Stress Intensity Factors. Inst. Fract. Solid Mech., Lehigh Univ., 1973.

17. Raju, I. S.; and Newman, J. C., Jr.: Three-Dimensional Finite-Element Analysis of Finite Thickness Fracture Specimens. NASA TN D-8414, 1977.

18. Isida, M.: Effect of Width and Length on Stress Intensity Factors of Internally Cracked Plates Under Various Boundary Conditions. Int. J. Fract. Mech., vol. 7, Sept. 1971, pp. 301-316.

TABLE I. - DIMENSIONLESS CRACK OPENING DISPLACEMENTS $Ev/\sigma_0 c$ AND DIMENSIONLESS y-DIRECTIONAL STRESSES σ_y/σ_0 FOR A RECTANGULAR BAR UNDER UNIFORM TENSION CONTAINING A THROUGH-THICKNESS CENTRAL CRACK
[ALL DATA IN y = 0 PLANE WITH ρ = CORRECTED CRACK EDGE DISTANCE.]

FINITE ELEMENT METHOD - REFERENCE 10 c = 1.0; W = 2.0; L = 1.75; t = 3.0; ν = 1/3				LINE METHOD c = 1.0; W = 1.92; L = 1.69; t = 2.90; ν = 1/3		
z	ρ	$\frac{Ev}{\sigma_0 c}$	$\frac{\sigma_y}{\sigma_0}$	ρ	$\frac{Ev}{\sigma_0 c}$	$\frac{\sigma_y}{\sigma_0}$
0	0.0132	0.3991	9.126	0.0132	0.384	8.975
	.0264	.5626	6.650	.0264	.541	6.552
	.040	.6910	5.381	.040	.666	5.599
	.080	.9698	3.852	.080	.937	3.996
	.120	1.1758	3.245	.120	1.142	3.330
	.160	1.3475	2.736	.160	1.314	2.912
	.200	1.4928	2.434	.200	1.463	2.602
	.400	1.9935	1.703	.400	2.023	1.888
	.600	2.3120	1.295	.600	2.390	1.320
	.920	------	-----	.920	2.640	.532
	1.000	2.5347	.531	1.000	2.651	-----
$\frac{t}{2}$	0.0132	0.4293	7.748	0.0132	0.441	8.463
	.0264	.6102	5.259	.0264	.622	6.121
	.040	.7552	4.046	.040	.766	5.030
	.080	1.0801	2.821	.080	1.081	3.667
	.120	1.3282	2.426	.120	1.321	3.048
	.160	1.5391	2.100	.160	1.524	2.664
	.200	1.7197	1.989	.200	1.679	2.392
	.400	2.3433	1.533	.400	2.385	1.678
	.600	2.7412	1.253	.600	2.830	1.210
	.920	------	-----	.920	3.140	.656
	1.000	3.0167	.703	1.000	3.157	-----

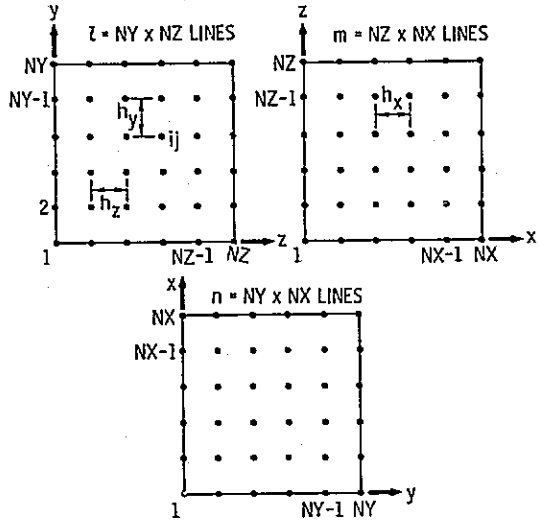

(a) THREE SETS OF LINES PARALLEL TO x-, y-, AND z-COORDINATES AND PERPENDICULAR TO CORRESPONDING COORDINATE PLANES.

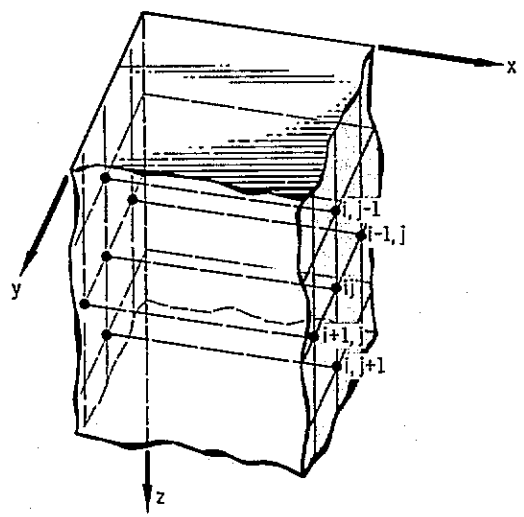

(b) SET OF INTERIOR LINES PARALLEL TO x-COORDINATE.

Figure 1. - Sets of lines parallel to Cartesian coordinates.

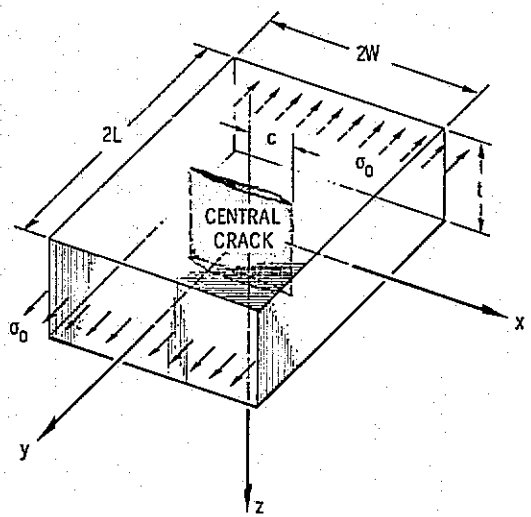

CS-70271

(a) RECTANGULAR BAR WITH THROUGH-THICKNESS CENTRAL CRACK.

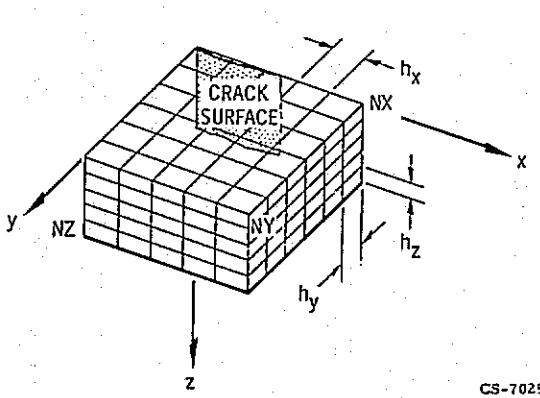

CS-70251

(b) DISCRETIZED REGION OF RECTANGULAR BAR WITH THROUGH-THICKNESS CENTRAL CRACK.

Figure 2. - Rectangular bar with through-thickness central crack under uniform tension.

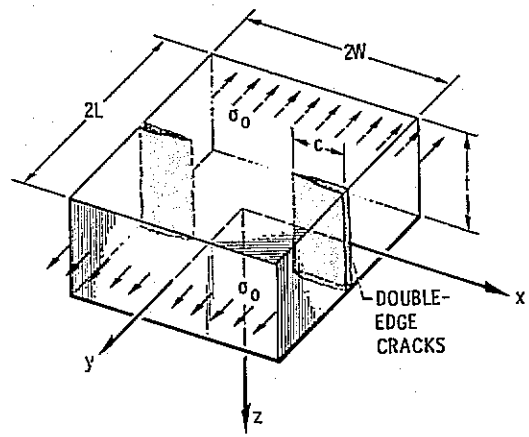

(a) RECTANGULAR BAR WITH THROUGH-THICKNESS DOUBLE EDGE CRACKS.

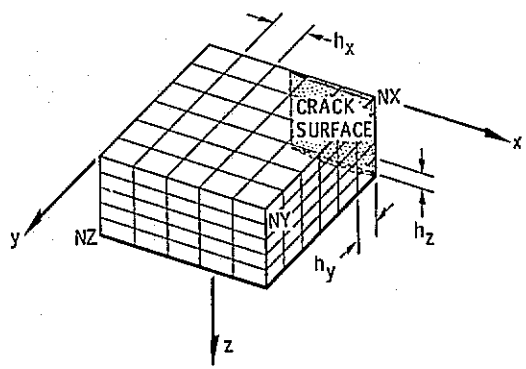

(b) DISCRETIZED REGION OF RECTANGULAR BAR WITH DOUBLE-EDGE CRACKS.

Figure 3. - Rectangular bar with through-thickness double-edge cracks under uniform tension.

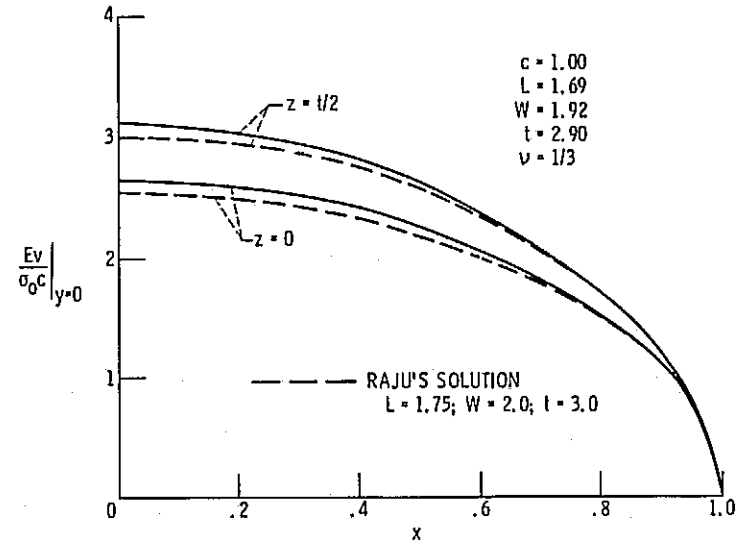

Figure 4. - Crack opening displacement for center-cracked bar under uniform tension.

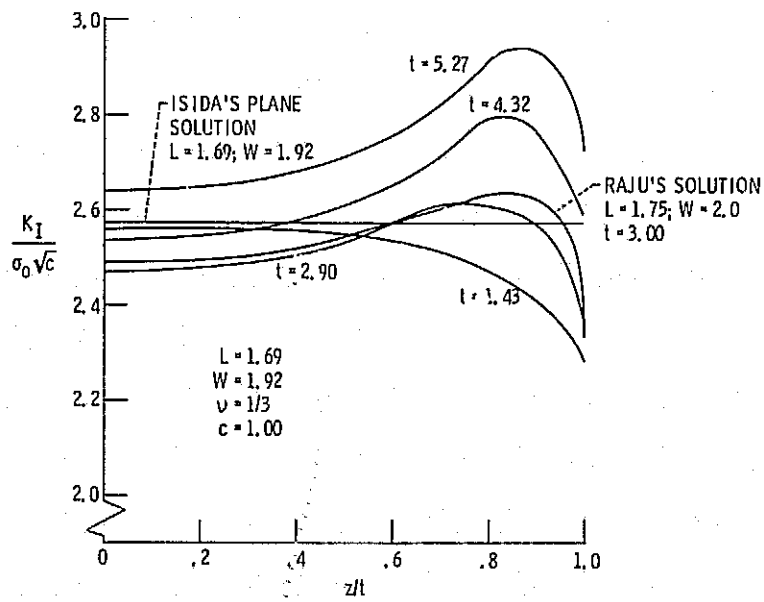

Figure 5. - Stress-intensity factor variation as a function of bar thickness for a center-cracked rectangular bar under uniform tension.

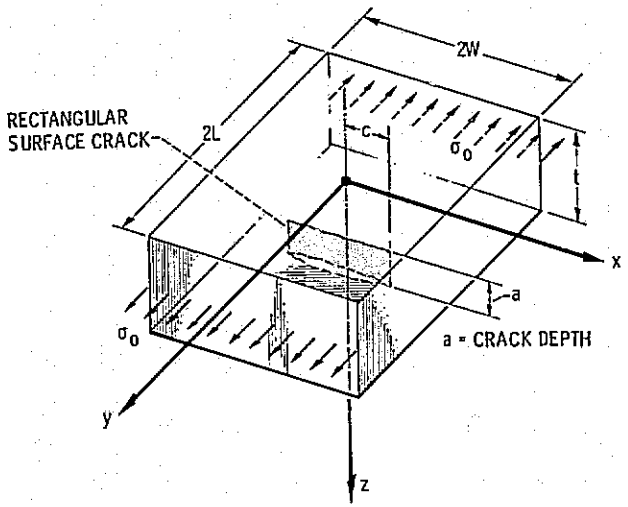

(a) BAR WITH RECTANGULAR SURFACE CRACK.

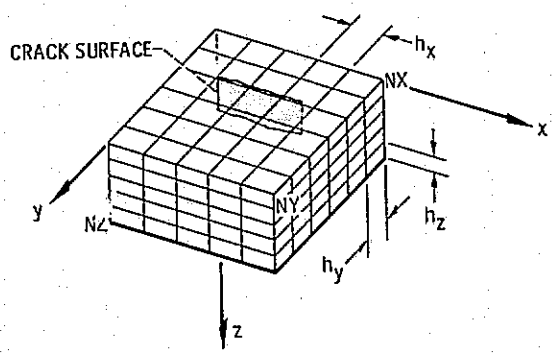

(b) DISCRETIZED REGION OF BAR WITH RECTANGULAR SURFACE CRACK.

Figure 6. - Bar with rectangular surface crack under uniform tension.

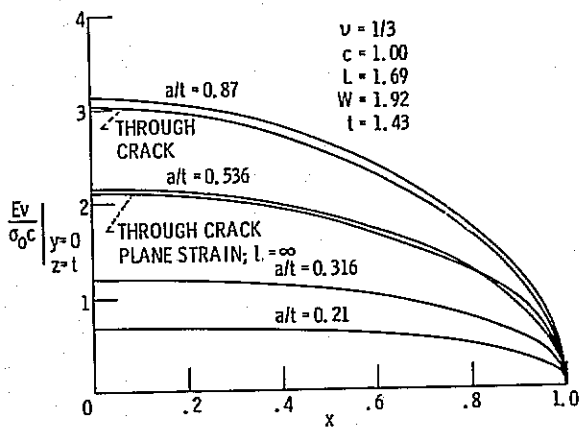

Figure 7. - Surface crack opening displacement variation as a function of crack depth for a rectangular bar under uniform tension.

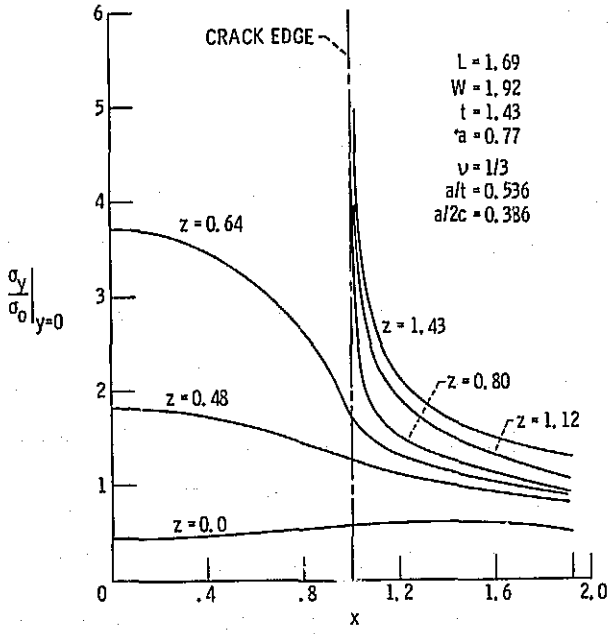

(a) DIMENSIONLESS y-DIRECTIONAL NORMAL STRESS VARIATION ALONG BAR WIDTH.

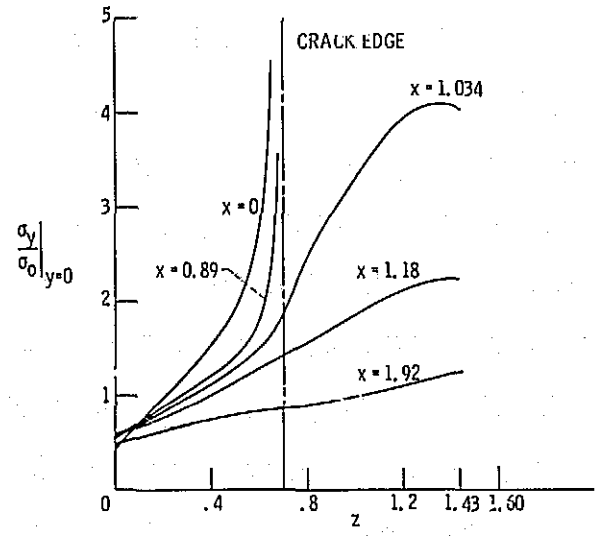

(b) DIMENSIONLESS y-DIRECTIONAL NORMAL STRESS VARIATION ACROSS BAR THICKNESS.

Figure 8. - Dimensionless y-directional normal stress distribution in the crack plane for a bar under uniform tension containing a rectangular surface crack.

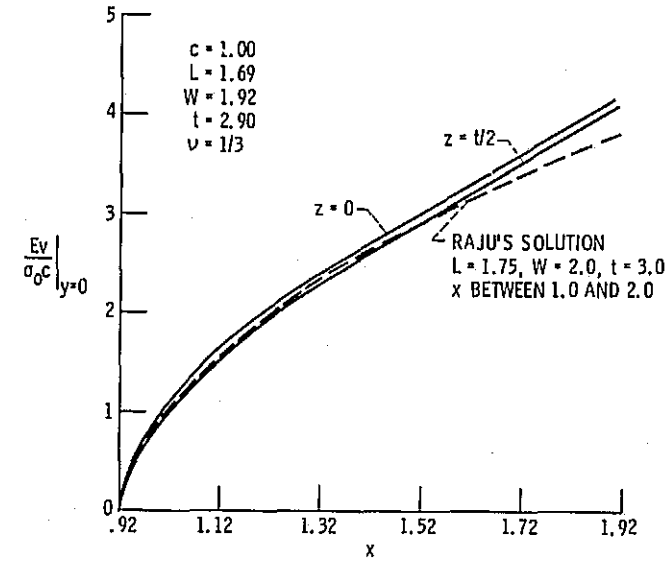

Figure 9. - Crack opening displacement for rectangular bar under uniform tension containing through-thickness double-edge cracks.

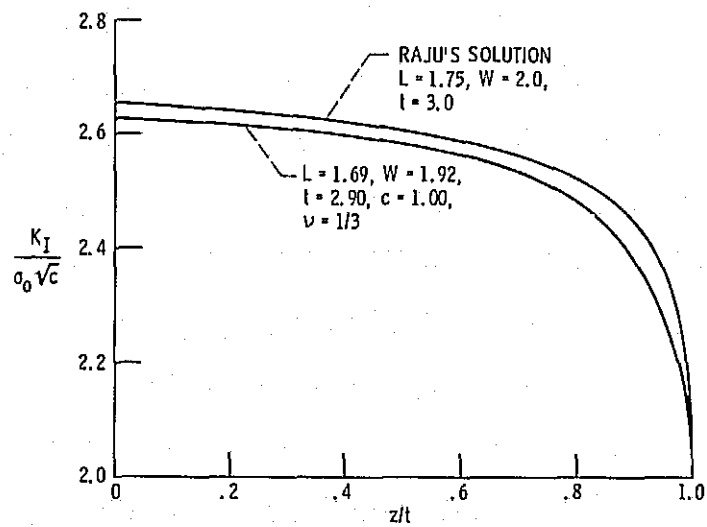

Figure 10. - Stress intensity factor variation as function of bar thickness for rectangular bar under uniform tension containing double-edge cracks.